IIE Transactions (2004) **36**, 237–251

ISSN: 0740-817X print / 1545-8830 online
DOI: 10.1080/07408170490274205

The analysis of feature-based measurement error in coordinate metrology

WENZHEN HUANG[1], ZHENYU KONG[1], DARIUSZ CEGLAREK[1] and EMILIO BRAHMST[2]

[1]*Department of Industrial Engineering, The University of Wisconsin-Madison, Madison, WI 53706-1572, USA*
E-mail: Darek@engr.wisc.edu
[2]*Center for Automotive Research, Ann Arbor, MI 48113, USA*

Received May 2002 and accepted May 2003

Coordinate measurement systems (CMSs) dominate the dimensional control and diagnostics of various manufacturing processes. However, CMSs have inherent errors caused by the lack of a tracing ability for some of the measured part features. This is important for product inspection and process variation reduction in a number of automated manufacturing systems, such as for example the automotive body assembly process. The lack of a feature tracing ability means that instead of measuring a given feature, the CMS may actually measure the area around the selected feature. In this paper, a principle for the part feature tracing ability and the resultant feature-based measurement error analysis are developed to estimate the aforementioned deficiencies in the CMSs. The impact of feature type and part(s) positional variation on the feature-based measurement error is explored. The proposed approach is applicable to both contact and non-contact CMSs including both mechanical and optical coordinate measuring machines. An analysis of the error for different measurement algorithms is presented. We show that the developed feature-based measurement error can have a significant impact on the measurement accuracy and hence on process control and the diagnostic algorithms currently used in manufacturing. A feature-based error map and error compensation approach are also developed and presented. Simulations, experimental results and two industrial case studies illustrate the proposed method.

1. Introduction

Dimensional measurements based on coordinate metrology (Coordinate Measurement System (CMS)) are widely used for product verification, process control and dimensional faults root causes diagnostics of various manufacturing processes. Computer-controlled mechanical and optical Coordinate Measuring Machines (CMMs) have become the dominant gages for dimensional measurement of mechanical parts. Recent developments in automotive and aerospace assembly have resulted in a rapid increase in the number of applications of coordinate gages for in-process product quality improvement and variation reduction. For example, a large number of automotive manufacturers have installed in-line optical CMMs in each of their main automotive body subassembly lines to measure every automotive body produced. These developments are compatible with the increased automation of manufacturing systems, which places high requirements on the reliability of measurement gages. The effectiveness of in-process control and quality improvements in complex manufacturing systems, such as multi-fixture sheet metal assembly is therefore critically dependent on the effectiveness of the measurements: throughput, accuracy, repeatability and reproducibility.

Recently, a significant amount of research has been conducted to improve the accuracy and throughput of coordinate dimensional gages (Hocken *et al.*, 1977; Hocken *et al.*, 1993; Wilhelm *et al.*, 2001). To a large extent the analysis of the accuracy of multi-axis coordinate machines is determined by: (i) geometric errors (Hocken *et al.*, 1977; Zhang *et al.*, 1985; Soons *et al.*, 1992; Yan *et al.*, 1999a, 1999b, 1999c); (ii) thermal errors (Bryan, 1990; Yuan and Ni, 1998); (iii) parametric errors (error related to motion of the individual elements of the measurement system) (Hocken *et al.*, 1993; Abbe *et al.*, 2000; Lee *et al.*, 2000); (iv) probe-related errors (Morgan *et al.*, 1984; Nawara and Kowalski, 1985; Estler *et al.*, 1996); (v) part-fixturing errors (Asada and By, 1985; Menassa and DeVries, 1989); and (vi) workpiece related errors (Salisbury and Peters, 1998). For example, Soons *et al.* (1992) presented a generalized model, which accounts for errors due to inaccuracies in the geometry, finite stiffness and thermal deformation of the machine's components in order to evaluate and optimize the calibration's efficiency. Their work was built on research done by Eman *et al.* (1987) and Bryan (1990). Additionally, sampling strategy, modeling substitute geometry of the feature being measured, and computational metrology were also intensively studied by Hocken *et al.* (1993) and Hopp (1993). Salisbury and Peters (1998) presented an error model for

prismatic parts that includes the prediction of workpiece location and orientation errors due to workpiece inconsistencies on datum planes. Moreover, Yan *et al.* (1999a, 1999b, 1999c) performed research on the uncertainty analysis and variation reduction of coordinate system estimation using discrete measurement data. This approach finds use in applications that deal with parts produced by end-milling processes and have a complex geometry. Lee *et al.* (2000) investigated issues of error identification and reduction in machine calibration and dimensional measurement using artifacts with geometric features in spherical form. Abbe *et al.* (2000) presented a method, which is able to describe the reliability of the parametric error as the calibration result of a CMM. Hernla (1997), Wilhelm *et al.* (2001) and Haitjema *et al.* (2002) developed techniques to model and estimate task specific uncertainty for CMSs, i.e., estimate error related to a specific measurement process plan.

The aforementioned research significantly improves the accuracy of mechanical and optical CMMs. In general, errors of dimensional measurement are analyzed either from the perspective of CMS equipment error, or of part locating fixturing error, as presented above. However, there exists an additional error related to the fundamental principle of coordinate measurement.

Currently, measurements conducted using CMSs may have inherent errors caused by the lack of a part feature tracing ability during the measurement process. The lack of a feature tracing ability means that instead of measuring the given feature, the CMSs may actually measure the area around the selected feature. In general, in the automotive industry, this is caused by the fact that CMSs measure a given part feature in one axis and assumed error free coordinates in other directions. CMSs do not have the capability to trace every measured feature on the part/subassembly and currently no algorithm exists to avoid such error(s) (Anon, 1988, 1992, 1994). CMSs offer only limited options to compensate for such potential measurement error sources by recalibration of the sensor (optical CMM) or by using various datum/reference coordinate systems. There is no algorithm or methodology that would compensate for the limited feature tracing ability of the CMSs. This deficiency is also not addressed in the recent CMS measurement literature (Bosch, 1995). Additionally, there is a paucity of research in the area of automotive assembly that analyzes the impact of the feature tracing limitations of the CMMs in relation to the applied measurement algorithm, measured feature, direction of the measurement and direction of the feature mislocation.

In the automotive industry mechanical and optical CMMs are commonly used for dimensional variation reduction for automotive body assembly. The measurement algorithms are set up to use the same coordinate system known as the body coordinate system. Figure 1 shows the coordinate axes and measurement features (marked reference points) in the body coordinate system (Ceglarek and Shi, 1995). These features are selected as Key Control Characteristics (KCCs). The measured data of KCCs reveals the geometrical/dimensional relationships between parts/subassemblies through multivariate statistical analysis (for example, correlation analysis and Principle Component Analysis (PCA)). The root cause of dimensional variations can thus be uncovered, for example the part/subassembly may have a rigid body movement, which can be identified by principal eigenvectors. Obviously there should be an assumption that exactly the same

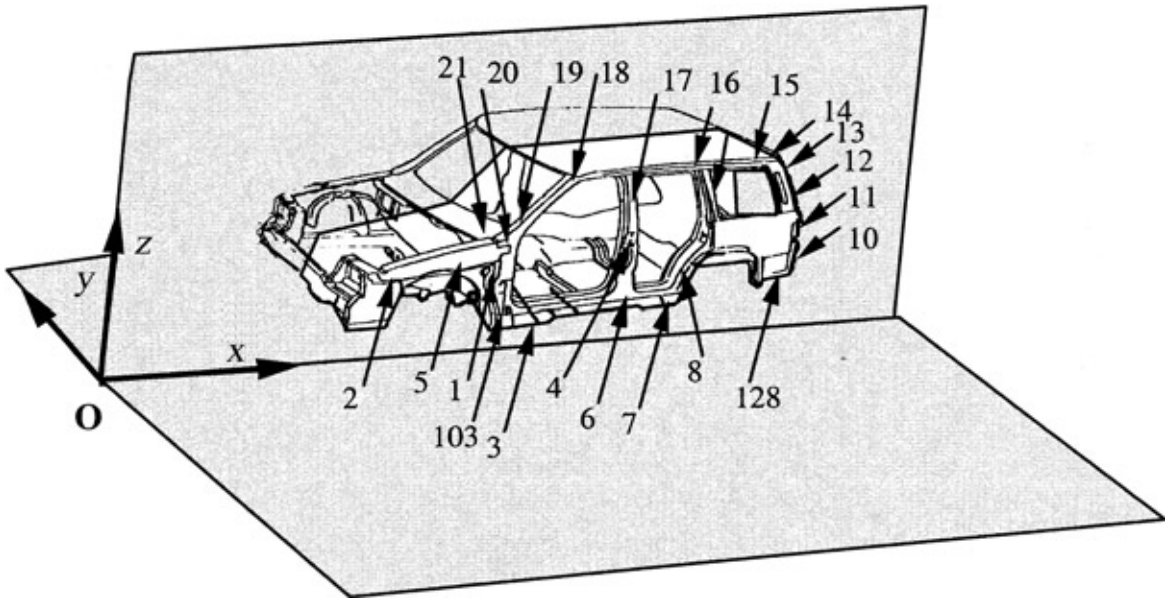

Fig. 1. The body coordinate system with an example of measurement point locations.

features have to be measured on different samples to avoid data inconsistency. Unfortunately, there is a mislocation of measured feature in 3-D and not just in the measured direction, which impose limitations on the current CMSs to trace and measure these intended features.

In a real situation the position and orientation of the measured part features are not exactly at the design nominals. This results in the part feature itself not being measured and instead a neighboring point being measured. It causes additional error in measurement which is additive to the other errors such as machine error or part fixturing error. This is especially important for in-process application of the coordinate measurement gages used for process control and improvement (variation reduction of the critical dimensions of the manufactured product) (Ceglarek *et al.*, 1994). The development of generic geometrical model-based variation simulation and diagnosis in multi-station manufacturing processes, especially in the automotive industry, challenges the state-of-the-art in coordinate metrology with regards to the part feature tracing ability during measurement of parts or subassemblies. For example, in the state space model of the dimensional variation propagation (Jin and Shi, 1999; Ding *et al.*, 2000), the state variables represented by part features need to be measured with respect to a local reference system, which implies that the feature needs to be traceable in the global coordinate system. The correct feature location information of a part/subassembly in the global coordinate system is important for correlation analysis and PCA used during root cause diagnosis of dimensional faults. These analyses are sensitive to the error described by the lack of feature traceability.

This paper presents a new analysis technique to quantitatively address and partially compensate for the aforementioned feature-based measurement error. The technique further improves upon the effectiveness of statistical calculations used for root cause diagnosis of dimensional variation (Ceglarek and Shi, 1996; Ding *et al.*, 2002a). It also enhances current research in the areas of variation reduction, in-process quality improvement and measurement system design (Nair *et al.*, 2000; Ding *et al.*, 2002b).

The paper is divided into seven sections. Section 2 presents the coordinate metrology based on the example of an automobile body assembly application. The feature-based measurement error, which results from the lack of a feature tracing ability in current measurement techniques, is described in Section 3. In Section 4, a feature-based measurement error map is presented. Experimental verification of the developed error model is shown in Section 5. Section 6 presents the impact of the error in the current industrial practice and a strategy for the feature-based measurement error compensation. Two case studies in the area of automotive body assembly process control and diagnostics illustrate the developed methodology and are also presented in Section 6. Finally, Section 7 summarizes results and draws conclusions.

2. Coordinate metrology

CMSs, including mechanical and optical CMMs, are widely used for off-line and in-process dimensional measurements of mechanical parts. These measurement systems allow the acquisition of accurate dimensional data on most part surfaces and readily record relationships between various part features. In-process CMMs are most often used for: (i) inspection (verification of dimensional deviations from design specifications or tolerances similar to the way it is done for off-line applications); and (ii) process control and improvement (dimensional analysis of product variation magnitude and patterns (product-to-product variation of measured features) that is especially critical for large volume production and affect not only part interchangeability but also product performance) (Ceglarek and Shi, 1995).

In general, CMMs are composed of one or more moving elements designed to position a measurement probe with respect to a part (Hocken *et al.*, 1993). It is recommended that the CMM probe approach the measured surface/feature in an orthogonal direction (Phillips, 1995; Estler *et al.*, 1996). The optical CMMs are usually also set up for measurement in a normal direction to the measured surface and can provide coordinates of the measured features. The measurement principles of the optical CMMs and the outline of the sensor setup for automotive body assemblies are described in Greer (1988).

The CMSs use measurement algorithms that take into account the number and locations of measurement points needed to estimate the position of the measured feature, and the direction of the approaching measurement points. Information included in the measurement algorithms should ensure that the probe can approach the nominal location of the measurement point. Furthermore, it is a common guideline in industrial practice to consider the direction of the approaching measurement points as being perpendicular to the measured surface (feature) in order to reduce any measurement error related to skidding (Phillips, 1995; Estler *et al.*, 1996). A CAD package usually provides all required design nominals and other geometrical information that is needed to set up the CMS measurement program.

A number of different algorithms are used to measure different geometrical features. For example, in the automotive body assembly process there are four major features measured on the product: (i) points; (ii) edges; (iii) holes; and (iv) slots. We now present a short description of the currently available algorithms for CMMs. Please refer to any CMM manual for detailed information (Anon, 1992).

Point feature algorithm (***Pick point with direction***): In general, a point measurement algorithm is used to measure a single point on the surface of a plane. It is intended to determine the height of a plane in a specified direction. The measurement direction is selected as a perpendicular to the measured surface. Although, the default measurement results of this algorithm can be x, y and z coordinates for

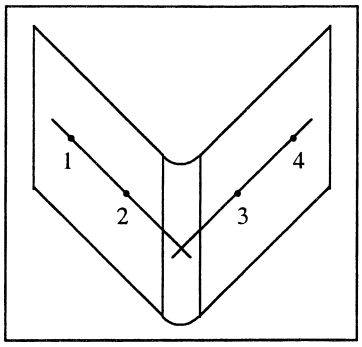

Fig. 2. An illustration of the use of the corner/edge feature algorithm.

the measured point, usually the axis which is the closest to the measurement direction will be the only one to be reported.

Corner/edge feature algorithm: Several different algorithms are used to determine locations of corner features.

1. By finding the intersection of two lines in space. For this purpose, a line is fit through two points measured on each side of the corner. The intersection of these lines determines the location of the corner (edge). Figure 2 illustrates this algorithm.
2. By measuring three points on each plane located on each side of the edge and then finding the line that is an intersection of these planes. The location of the measurement point is determined by the nominal position on the constrained axis of the intersecting lines.

Measurement data are usually reported along the two axes closest to the perpendicular directions of the intersection line.

Hole/slot feature algorithm: Several different algorithms are used to determine the location and size of hole/slot features, which may require measuring between three and 100 points. As an example, the hole/slot feature algorithm can be divided into four steps (Fig. 3): (i) finding the rough location of the hole/slot; (ii) determining the hole/slot location; (iii) determining the hole/slot plane; and, (iv) measuring the hole/slot size. Each step can be performed with a different set of measurements. For instance, steps 3 and 4 can be realized as follows; three points are picked on the surface around the feature to determine the accurate position of the plane with the hole/slot (step 3). Then the measurement is taken by picking four points on the perimeter and by a calculation of the precise position and dimension of the hole/slot (step 4). Figure 3 summarizes the entire algorithm for a hole. The reported measurement of the hole/slot algorithm is the x, y and z coordinates of the measured hole/slot.

3. Feature-based measurement error

Measurements conducted by CMSs have inherent errors caused by the lack of a tracing ability for some of the measured features, which means that instead of measuring the given feature, the CMS may actually measure the area around the feature. This inherent error related to the method of coordinate measurement can be caused by many factors and can include combinations of part-positioning error, part geometry and direction of measurement. The part-positioning error is the result of errors related to assembly or measurement fixture, part fabrication (for example, machining or stamping processes) and part-to-part joining processes (for example, welding and riveting). A part has translational error and angular error. However, the angular error can be ignored since, based on industrial experience, even in the worse case the angular error is less than 0.008 rad. Additionally, following industrial practice, we assume that the direction of the measurement is always perpendicular to the measured feature. Figure 4 illustrates the described feature-based measurement error based on the CMM measurement of a point on a plane. The part mislocation (mislocation of the measurement point A in the z direction) causes a measurement error in the y direction (Fig. 4). The measured point A** is not the feature that was intended to be measured (A*). However, due to the lack of a feature tracing ability of the coordinate measurement system, instead of point A*, point A** is measured with an inherent error in addition to the other errors related to the accuracy of the measurement device. This will now be explained in more detail.

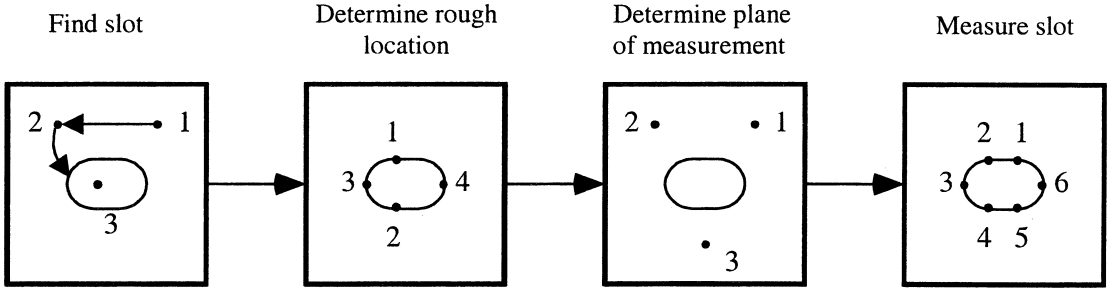

Fig. 3. An illustration of the use of the hole/slot feature algorithm.

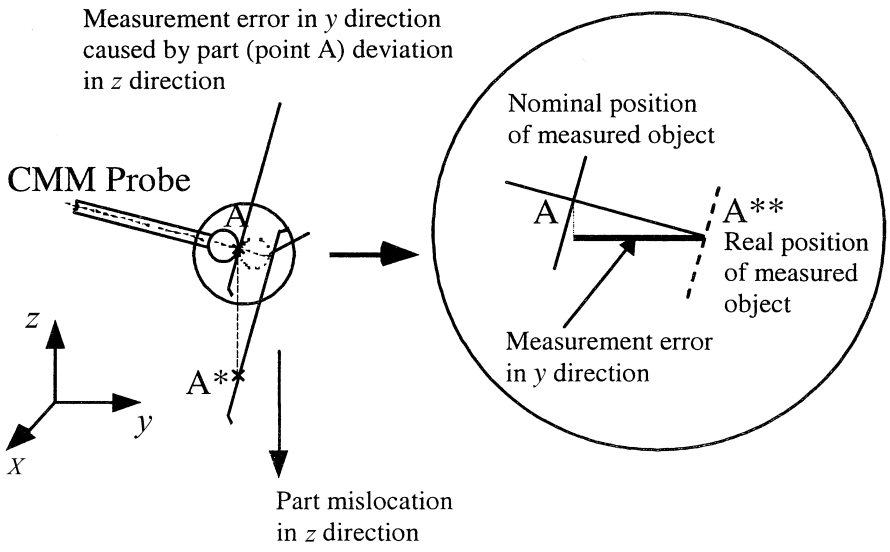

Fig. 4. A schematic diagram of the error in the y direction caused by a part mislocation in the z direction. A—nominal position of the measurement point; A*—mislocated position of the measurement point caused by part mislocation in z direction; and A**—point measured.

The analysis of the feature-based measurement error is discussed based on the measurement of three basic features presented in Fig. 5: (i) square/hole/slot; (ii) edge; and (iii) plane.

Definition 1. The feature tracing ability of the ideal (error-free) measurement system is its inherent ability to measure the location of a given feature in the selected direction.

The feature tracing ability describes feature-based measurement errors caused by the inability of the system to measure the intended point/feature due to part/subassembly positioning error or part/subassembly geometrical error (see Fig. 4, the point intended to be measured A* as opposed to the actually measured point A**). The feature tracing ability, as presented in this paper, is not related to the total error of the measurement system. Rather it is related to the lack of capability of the system to measure the feature, reflected by measurement of the neighboring area around the feature instead of the feature itself. For CMSs such as mechanical and optical CMM systems, the following classification of feature tracing ability is proposed:

1. Level 1: a feature traceable in three directions (fully traceable feature) such as the square, hole or slot shown in Fig. 5(a). These are features that can be accurately traced by a measurement system, so that the total measurement

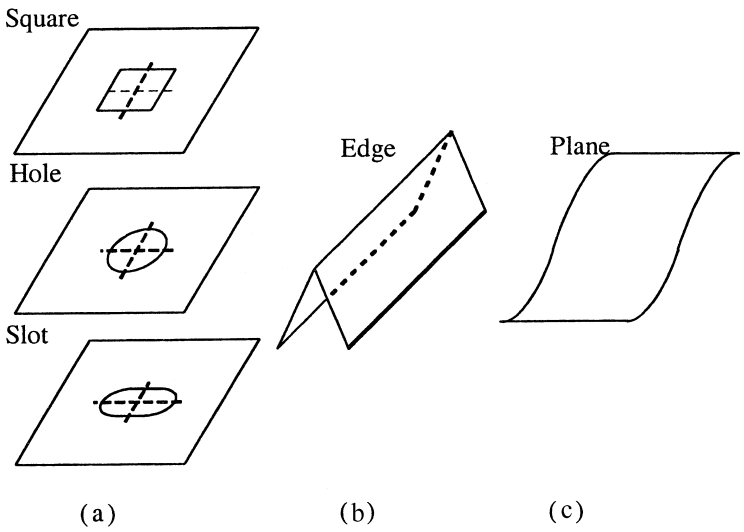

Fig. 5. A schematic diagram of the three selected measurement features: (a) square/hole/slot; (b) edge; and (c) plane.

error does not include the feature-based measurement error (see algorithm described in Section 2).
2. Level 2: a feature traceable in two directions (feature traceable in one plane) such as the edge shown in Fig. 5(b). These are features that can be accurately traced by a measurement system in one plane, called the further tracing plane (two directions). Feature mislocation in the tracing plane does not affect the error of the ideal measurement system.
3. Level 3: a feature traceable in one direction such as the point on plane shown in Fig. 5(c). These are features that can be accurately traced by a measurement system in one direction, called the further tracing direction. Feature mislocation in the tracing direction does not affect the error of the ideal measurement system.

The phenomena of feature tracing ability can be summarized as follows:

Principle of feature-based measurement error: The measurement of a part/subassembly feature by an ideal (error-free) CMS can generate inherent error, which can be determined based on the level of feature tracing ability and direction of measurement.

The magnitude of the error of the ideal CMS, which is related to the system feature tracing ability, depends on: (i) the direction of measurement; (ii) the feature geometry; and (iii) the direction/pattern of the feature variation. These relations for linear feature variation are presented by Theorem 1.

Theorem 1. *The relationships between the level of the feature tracing ability and the feature-based measurement error* $\boldsymbol{e}(x, y, z)$ *can be described as follows*:

1. *Level 1*: *feature traceable in three directions* (*fully traceable feature*):

$$e_1(x) = 0, \quad e_1(y) = 0, \quad e_1(z) = 0, \tag{1}$$

where e is the feature-based measurement error along each coordinate axis.

2. *Level 2*: *feature traceable in two directions*:

$$e_2(x) = 0, \tag{2}$$
$$e_2(y) = d_z^* \sin\alpha\cos\alpha - d_y^* \sin^2\alpha, \tag{3}$$
$$e_2(z) = d_y^* \sin\alpha\cos\alpha - d_z^* \cos^2\alpha, \tag{4}$$

where d_y^*, *and* d_z^* *is the deviation of the feature in the y and z direction respectively* (*Fig. 6*).

3. *Level 3*: *feature traceable in one direction*

$$e_3(x) = d_x^*(\cos^2\alpha\sin^2\beta - 1) + d_y^*(\cos^2\alpha\sin\beta\cos\beta) + d_z^*(\sin\alpha\cos\alpha\sin\beta), \tag{5}$$
$$e_3(y) = d_x^*(\cos^2\alpha\sin\beta\cos\beta) + d_y^*(\cos^2\alpha\cos^2\beta - 1) + d_z^*(\sin\alpha\cos\alpha\cos\beta), \tag{6}$$
$$e_3(z) = d_x^*(\sin\alpha\cos\alpha\sin\beta) + d_y^*(\sin\alpha\cos\alpha\cos\beta) + d_z^*(\sin^2\alpha - 1), \tag{7}$$

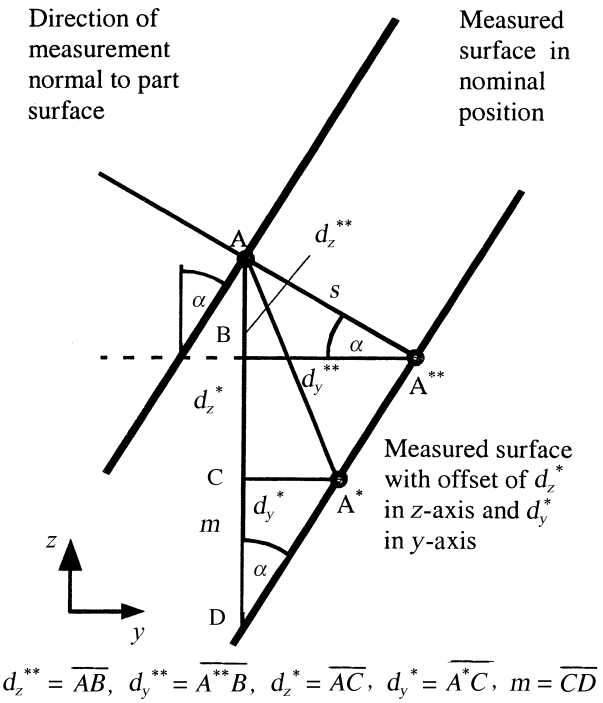

Fig. 6. Feature 2 level: geometrical relations for feature-based measurement error.

where, d_x^*, d_y^* *and* d_z^* *are the deviations of the feature in the x, y and z directions respectively.* α *and* β *are the angles between the intersection lines* (*between a part's surface and coordinate planes*) *and the coordinate axes as defined in Fig. 7.*

Proof for level 2 features. The feature-based measurement error at level 2 is shown in Fig. 6. The feature's deviation is determined by:

$$d_y^{**} = s\cos\alpha, \tag{8}$$
$$d_z^{**} = s\sin\alpha. \tag{9}$$

where s is the distance AA**. In Equations (8) and (9), s can be substituted by:

$$s = (d_z^* + m)\sin\alpha, \tag{10}$$
$$m = \frac{d_y^*}{\tan\alpha}. \tag{11}$$

The feature-based measurement error is the distance between the measured feature (A**) and the actual position of the feature (A*). Equations (12) and (13) describe these error components in the y and z directions, and they are obtained by substituting Equations (8)–(11) into the definition of $e_2(y)$ and $e_2(z)$.

$$e_2(y) = d_y^{**} - d_y^* = d_y^*\cos^2\alpha + d_z^*\sin\alpha\cos\alpha - d_y^* = d_z^*\sin\alpha\cos\alpha - d_y^*\sin^2\alpha, \tag{12}$$
$$e_2(z) = d_z^{**} - d_z^* = d_y^*\sin\alpha\cos\alpha + d_z^*\sin^2\alpha - d_z^* = d_y^*\sin\alpha\cos\alpha - d_z^*\cos^2\alpha. \tag{13}$$

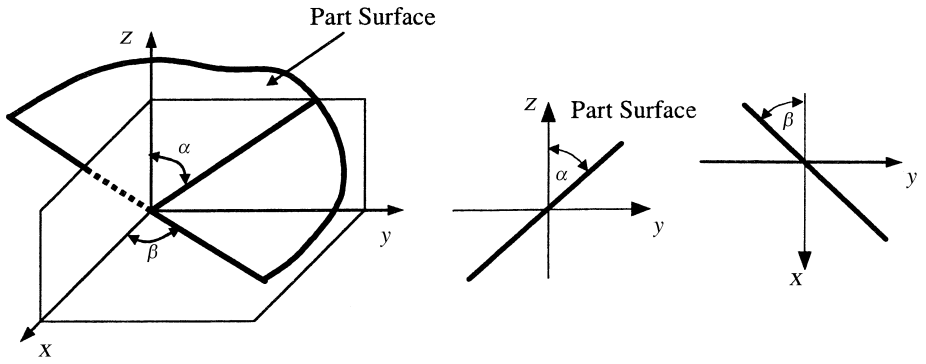

Fig. 7. Definition of angles for feature on measurement object.

Equations (12) and (13) are equivalent to Equations (3) and (4).

Proof for level 3 features. The error for the three-dimensional case can be described as a vector **e**. Assume that $\mathbf{d}^*$ is the part displacement vector, and **n** is the unit normal vector of the part surface. Therefore, vector **e** represents the difference between the displacement vector $\mathbf{d}^*$ and the projection of $\mathbf{d}^*$ onto **n**, as shown in Fig. 8.

The projection of $\mathbf{d}^*$ onto the normal axis of the part may be obtained by using matrix $\mathbf{P_n}$:

$$\mathbf{P_n} = \frac{\mathbf{n}\mathbf{n}^T}{\mathbf{n}^T\mathbf{n}} = \mathbf{n}\mathbf{n}^T \quad \text{for } \|\mathbf{n}\| = 1. \tag{14}$$

The error vector **e** is then defined as:

$$\mathbf{e} = \mathbf{P_n}\mathbf{d}^* - \mathbf{d}^* = (\mathbf{P_n} - \mathbf{I})\mathbf{d}^* = (\mathbf{n}\mathbf{n}^T - \mathbf{I})\mathbf{d}^*. \tag{15}$$

According to Fig. 9, the normal unit vector can be described as:

$$\mathbf{n} = \begin{bmatrix} \cos\alpha \sin\beta \\ \cos\alpha \cos\beta \\ \sin\alpha \end{bmatrix}. \tag{16}$$

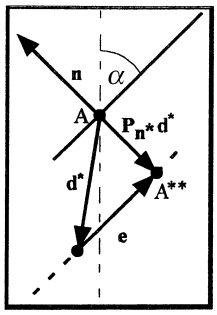

Fig. 8. Feature 3 level: geometric relations for feature-based measurement error. **n**—unit measurement vector (perpendicular to the measured surface); $\mathbf{d}^*$—part displacement vector; and **e**—feature-based measurement error.

The total error is shown below as:

$$\mathbf{e} = \begin{bmatrix} e_3(x) \\ e_3(y) \\ e_3(z) \end{bmatrix} = (\mathbf{n}\mathbf{n}^T - \mathbf{I})\mathbf{d}^*$$

$$= \begin{bmatrix} \cos^2\alpha \sin^2\beta - 1 & \cos^2\alpha \sin\beta \cos\beta & \sin\alpha \cos\alpha \sin\beta \\ \cos^2\alpha \sin\beta \cos\beta & \cos^2\alpha \cos^2\beta - 1 & \sin\alpha \cos\alpha \cos\beta \\ \sin\alpha \cos\alpha \sin\beta & \sin\alpha \cos\alpha \cos\beta & \sin^2\alpha - 1 \end{bmatrix} * \begin{bmatrix} d_x^* \\ d_y^* \\ d_z^* \end{bmatrix}. \tag{17}$$

Equation (17) is equivalent to Equations (5)–(7).

3.1. *Discussion*

The presented feature-based measurement error is related to and extends the research conducted in the areas of measurement traceability and task-specific measurement uncertainty by providing insights into what could be called feature-based metrology:

1. The *task-specific uncertainty* is defined as the measurement uncertainty associated with the measurement of a specific feature using a specific measurement plan (Hernla, 1997; Wilhelm *et al.*, 2001; Haitjema *et al.*, 2002).
   Task-specific uncertainty discusses error related to a specific measurement process plan. The magnitude of

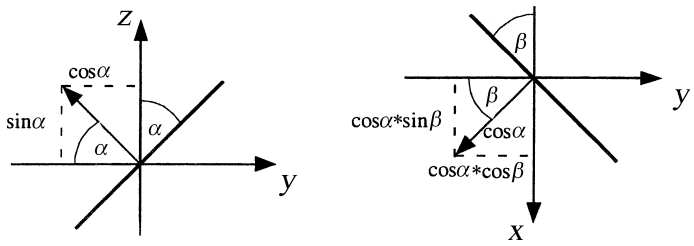

Fig. 9. Position of normal vector on part surface.

the currently presented feature-based error is affected by a specific measurement plan/tasks, but the concept of the error itself is rather independent of it. The presented feature-based measurement error is not exactly related to the specific inspection plan but rather it is inherently related to the fundamental principles of the coordinate measurements. The error presented in this paper can provide one of the building blocks for task-specific uncertainty.

2. *Traceability* (ISO)-property of the result of a measurement or the value of a standard whereby it can be related to stated references, usually national or international standards, through an unbroken chain of comparisons all having stated uncertainties (Anon, 1995).
   The presented feature-based error analysis can add a missing link to the traditional traceability chain by providing insights into the feature tracing ability of the CMSs.

Additionally, the dimensional measurements are commonly used for:

1. Dimensional analysis of *product deviation from designs nominal(s)*. For example, evaluation of profile tolerance or just simple estimation of dimensional tolerances for a set of selected and independent measurement points.
   The presented error definition and mathematical formulation has a limited impact on the evaluation of a three-dimensional profile tolerance for those cases that have a shift of the entire datum surface(s), for example, for features when the α angle (shown in Fig. 7) is the same for all measured points on that feature. However, in cases of some non-linear features, the shift of the surface (datum) in the y and/or z direction can affect the profile tolerance. This occurs when the error for each measured point caused by the feature shift changes, with a different magnitude for different points. This can occur due to a different orientation of a point and its neighborhood area (for example when the α angle (shown in Fig. 7) is not the same for all measured points on a given feature). The presented error will occur for features which require multi-point measurement with a varying α angle for each point.
2. Dimensional analysis of *product variation magnitude and patterns* (product-to-product variation of measured features). This is especially critical for large volume production and affects not only part interchangeability but also product performance. The dimensional variation of a product has two unique characteristics:
   (i) The measured multi-part products are made from a number of parts, with datum and measurement points located often on different parts. This gives rise to an inherent error with a varying magnitude between the datum and measurement points in all directions and not just in the measured direction. This is one of the main reasons for the error analysis described in this paper.
   (ii) The variation error is estimated by measurement of a given sample or, often used in the automotive industry, of a 100% of the produced/assembled products. Each measured product varies dimensionally, which means that the error described in this paper has a varying magnitude and as a result, directly affects the accuracy of the measurements.

4. Map of feature-based measurement error

The importance and impact of the feature-based measurement error is shown by conducting simulations based on the relations developed in Section 3. Simulations are conducted for level 3 features, which are traceable in one direction. Simulations for level 2 features can be conducted in similar way. The presented simulation will be conducted in five series according to the outline presented in Table 1.

Additionally, each simulation series is conducted for different orientations of part features, as defined by the angles α and β (Fig. 7). Both the α and β angles are varied between 0° and 30° and the sample size used for variation range is 100.

Simulation series 1 and 2: Figure 10 (a and b) shows the results of the feature-based measurement error for part deviation along the z-axis (Fig. 10(a)) and also the part variation along the z-axis (Fig. 10(b)). Since part mislocation is

Table 1. Outline of the conducted simulations

	Part feature deviations (1 mm from nominal) along			*Part feature variation (±0.5 mm) along*			
Simulation series	*y-axis*	*z-axis*	*x-, y-, z-axis*	*y-axis*	*z-axis*	*x-, y-, z-axis*	
1		x					Fig. 10(a), Table 2
2					x		Fig. 10(b), Table 2
3	x						Fig. 11(a)
4				x			Fig. 11(b)
5			x				Fig. 12

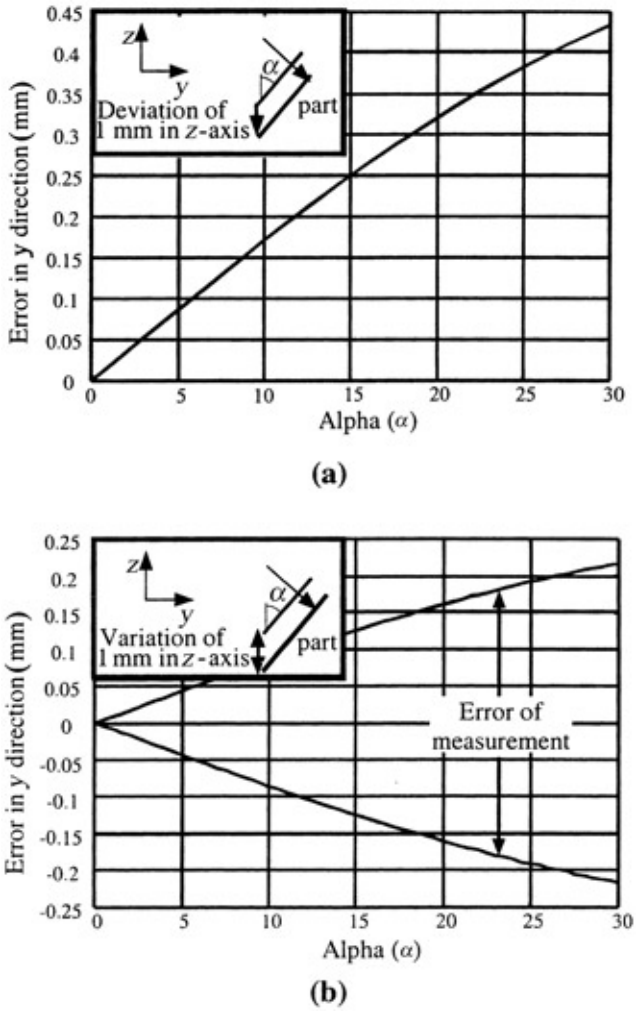

Fig. 10. Feature based measurement error for: (a) part deviation; and (b) part variation of the z-axis and $\alpha = \langle 0, 30^\circ \rangle$.

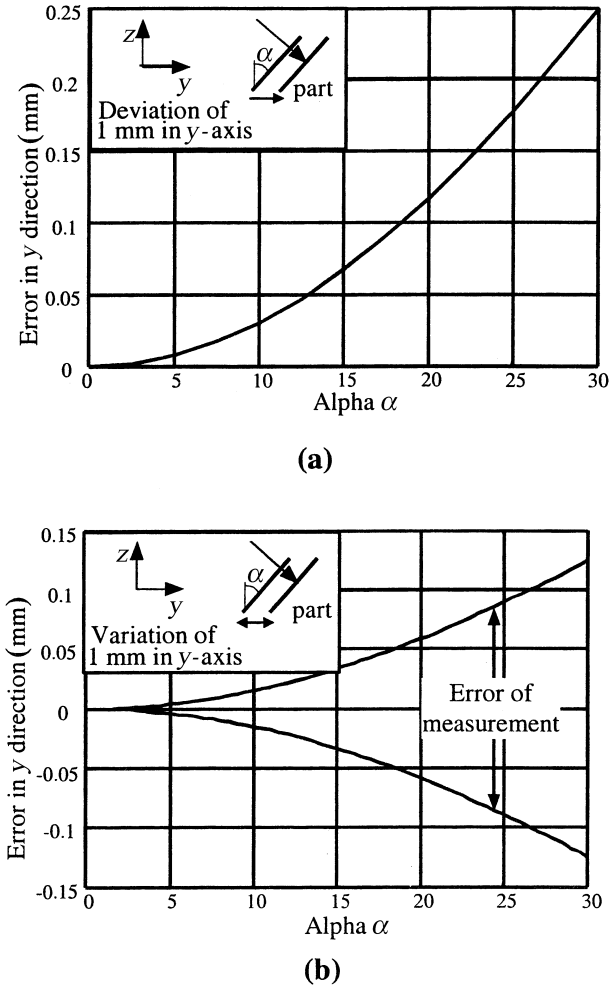

Fig. 11. Feature-based measurement error for: (a) part deviation; and (b) part variation of the y-axis and $\alpha = \langle 0, 30^\circ \rangle$.

assumed to be 1.0 mm, the resulting error when multiplied by 100 can be interpreted as the percentage impact of the part deviation or variation on the feature-based measurement error.

It can be concluded from Fig. 10(a) that the relative feature-based measurement error can reach up to 43% of the part deviation error when $\alpha = 30^\circ$. For a part deviation of 1 mm in the z direction, a feature-based measurement error in the y direction is equal to 0.43 mm.

Simulation series 3 and 4: Figure 11 (a and b) shows the results of the feature-based measurement error calculation for part deviation along the y-axis (Fig. 11(a)), and also the part variation along the y-axis (Fig. 11(b)). As in the previous simulation series 1 and 2, the part mislocation is 1.0 mm. The relative feature-based measurement error in the y direction reaches up to 25% of the measured part deviation or variation in the y direction ($\alpha = 30^\circ$).

Simulation series 5: The results of the error calculations for simultaneous part deviation in the x, y and z directions are shown in Fig. 12. The part mislocation is 1.0 mm in all axes. Figure 12 shows that the feature-based measurement error can reach up to 1.1 mm for a given deviation of 1 mm in each axis, and $\alpha = \beta = 30^\circ$. Figure 12 can also be used as the feature-based measurement error map, which shows the magnitude of the errors for different feature orientations as a function of the direction of measurement.

The understanding of the feature-based measurement error can help to compensate the error, for example: (i) by creating an error map for a given product (as shown in Fig. 12); (ii) by developing a special sensor placement procedure with the capability to suppress the error; or (iii) by developing a strategy for feature-based measurement error compensation (Section 6).

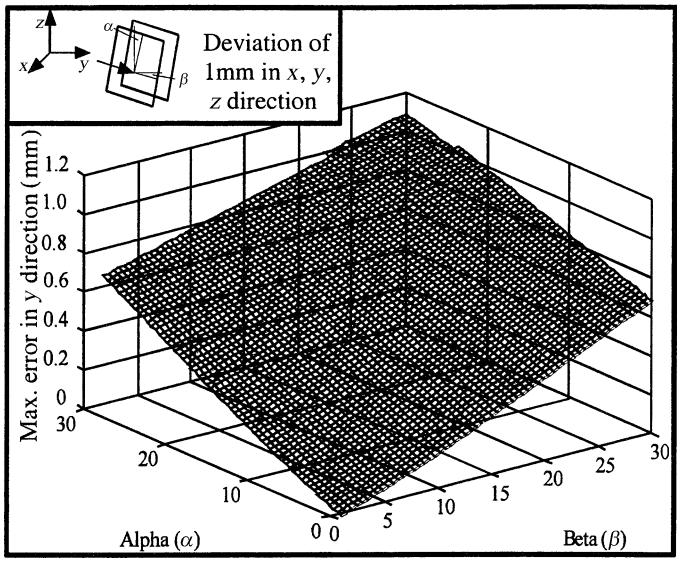

Fig. 12. Feature-based measurement error for simultaneous part deviation in the x, y and z axes and α, $\beta = \langle 0, 30^\circ \rangle$.

5. Verification of the feature-based measurement error model

This section presents experimental verification of the proposed feature-based measurement error model.

To verify the model, a block with plane surfaces was fixed on a Sheffield CMM table using a fixture that is adjustable in four directions: translations in the x and y axes and rotations around the x and z axes (Fig. 13). The coordinates of the center point and the normal vector of the plane were found by measuring three points on the surface. Offsetting the probe from the center point by selected deviations simulates the occurrence of the feature-based measurement error if the part is again measured at this point. The difference between these measurements in the x, y and z directions indicates the error for a given part position and deviation. Figure 13 shows the experimental setup.

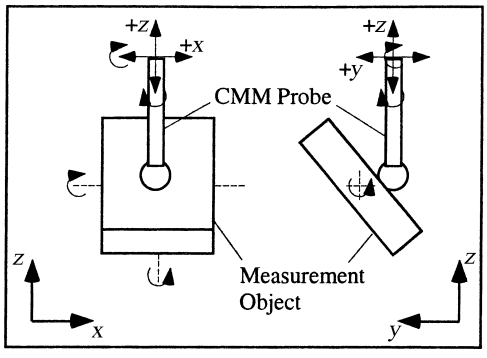

Fig. 13. Experimental setup.

Experiments followed the outline presented in Table 1 and were conducted at various positions of the part for different amounts of deviation in the x, y and z directions (the deviations range from 0 to 3 mm). The differences between the measured values and those calculated using the developed feature-based measurement error model were within the 0.01 mm range, which is the equivalent of the inherent accuracy of the mechanical CMM used in these experiments.

6. Impact of the measurement error in current industrial practice and strategy for error compensation

6.1. *Impact of the measurement error*

This section presents the impact of the feature-based measurement error for a point feature (level 3), as described by Equations (5)–(7). Table 2 summarizes the total feature-based measurement error for a point feature measurement assuming the following conditions: (i) the α varies from 0° to 30° (y-z plane) and β is zero (x-y plane); (ii) the measurement is reported in the y direction; and (iii) the variation of the measured feature is 1.0 mm in the z direction (z is the non-measured direction).

Table 2 shows that the feature-based measurement error depends on the relative orientation of the measured feature and the direction of the part variation/deviation from the design nominal (as described by α), as well as on the underlying part variation magnitude. It also shows that only those point features, which are located in a plane parallel to a plane of the coordinate system ($\alpha = \beta \cong 0$), does not have any measurement error as described by the feature tracing principle.

Table 2. Feature-based measurement error in y direction for part variation in z-axis

Surface angle α	*Part variation in z direction (mm)*	*Measurement error in y direction (mm)*	*Measurement error in y direction (%)*
0.0	1.0	0.00	0
2.0	1.0	0.03	3
4.0	1.0	0.07	7
6.0	1.0	0.10	10
8.0	1.0	0.14	14
10.0	1.0	0.17	17
12.0	1.0	0.20	20
14.0	1.0	0.23	23
16.0	1.0	0.27	27
18.0	1.0	0.29	29
20.0	1.0	0.32	32
22.0	1.0	0.35	35
24.0	1.0	0.37	37
26.0	1.0	0.39	39
28.0	1.0	0.41	41
30.0	1.0	0.43	43

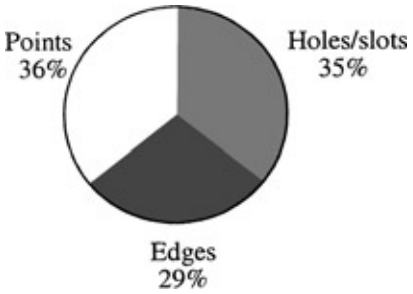

Fig. 14. Measurement point features distribution for industrial case study 1.

6.1.1. *Industrial case study 1*

To evaluate the significance of the analyzed error, an industrial case study was conducted for an automotive body assembly process in one of the US automotive manufacturers. The automotive bodies are inspected in-line during the assembly process by an optical CMM as well as off-line by a mechanical CMM at 45 measurement points. Each measurement point was classified according to its feature type and level number, and modeled based on the CAD data (feature type, location coordinates and α and β angles). Then, the feature-based measurement error was calculated by applying Equations (5)–(7). The following results were obtained. Out of the total of 45 measurement points on the automotive bodies, there are 16 (35.5%) point measurements (feature level 3) (Fig. 14). For eight (50%) of these points, the feature-based measurement error exceeds 4% of the observed deviation in the non-measured direction and for two (12%) of these points, the feature-based measurement error exceeds over 44% of the variation in the non-measured direction. Figure 15 shows the relative feature-based measurement error for point feature measurements on the studied automotive body.

It was also identified that 20% of the all measurement points have a feature-based measurement error of more than 4% for any measured deviation or variation in the non-measured directions.

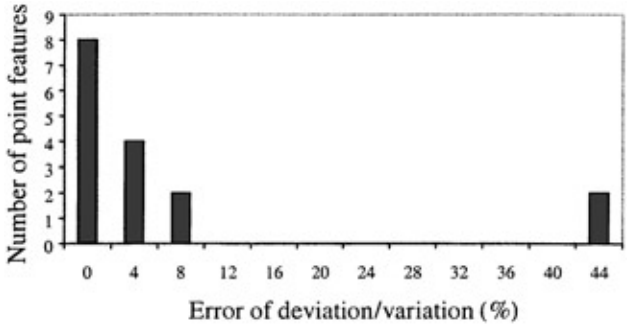

Fig. 15. Industrial case study 1: feature-based measurement error for automotive body measurement points (point features are level 3 features).

6.2. *Strategy for compensation of the feature-based measurement error*

As presented in the previous sections the feature-based measurement error can have a significant impact on the accuracy and precision of the dimensional data gathered on a product, which are used for product inspection or manufacturing process control or equipment calibration. Furthermore, the feature-based measurement error also affects the results of measurement data analysis in currently used methodologies related to:

1. Dimensional analysis of product deviation from designs nominal(s). For example, evaluation of profile tolerance or just simple estimation of dimensional tolerances for a set of selected and independent measurement points.

   The presented error definition and mathematical formulation has limited impact on the evaluation of a three-dimensional profile tolerance for some cases with "shift of the entire datum surface(s)"; for example, for features when the α angle (Fig. 7) is the same for all measured points on that feature. However, feature-based measurement error affects the evaluation of a 3-D profile tolerance in cases when the error for each measured point caused by a feature shift changes, with a different magnitude for different points. This can occur due to a different orientation of a point and its neighborhood area/subfeatures (for example when the α angle is not the same for all measured points on a given feature). The presented error will occur for features which require multi-point measurement with a varying α angle for each point.
2. Dimensional analysis of the product variation magnitude and patterns (product-to-product variation of measured features). This is especially critical for large volume production and can affect not only part interchangeability but also product performance. (Hu and Wu, 1992; Ceglarek and Shi, 1995; Ceglarek, 1998; Ding *et al.*, 2002c). The methods of root cause isolation of dimensional variation faults are based on the correlation analysis and the calculation of eigenvector/eigenvalue pairs to estimate variation patterns. Both the correlation and eigenvalue/eigenvectors are sensitive to feature-based measurement error. The dimensional variation of the product has two unique characteristics:

   (i) The measured multi-part products are made from a number of parts with datum and measurement points often located on different parts. This gives rise to inherent error with a varying magnitude between the datum and measurement points in all directions and not just in the measured direction. This is one of the chief reasons for the error analysis described in this paper.

(ii) The variation error is estimated by measurement of a given sample, or as often used in automotive industry, of a 100% of the produced/assembled products. Each measured product varies dimensionally, which causes the error described in this paper to have a varying magnitude and as a result this directly affects the accuracy of the measurements.

3. Multi-stream process (multiple tooling process) adjustments (Montgomery, 1997). Currently, the most often used methods for multiple tooling adjustments depend on the indirect measurement of a product to determine the adjustment level of the production tooling.

This paper does not present a quantitative analysis of the impact of feature-based measurement error on the aforementioned methods. However, there is a strong need for a comprehensive analysis and guidelines to eliminate or fully/partially compensate for the feature-based measurement error. Additionally, an understanding and analysis of the feature-based measurement error can lead to the selection of measurement point locations (sensor layout optimization; measurement feature selection) during the early design phase of the new product/process development.

The general strategy for elimination or compensation of feature-based measurement error can be presented in the following steps:

Step 1. Select fully traceable features as measurement points (level 1-holes/slots) which do not cause any feature-based measurement error.

Step 2. If selecting partially traceable features (levels 2 or 3):

(a) Measure only a traceable direction (level 2)
(b) If measurements of non-traceable directions of a given feature are necessary follow the feature-based measurement error compensation approach.

6.2.1. *Feature-based measurement error compensation approach*

Feature-based measurement error can be estimated based either on CAD information about the measured feature; or on measurement data of the feature positioning error in non-measured direction(s). Therefore, the compensation of feature-based measurement error of a given non-fully traceable measurement point A(x, y, z), with either measurement direction i, or non-traceable direction(s) j for level 2, or j and k for level 3, can be conducted in the following manner.

Step 1. Selection of traceable measurement point T(x, y, z), which does not have the feature-based measurement error in the non-measured direction of the point A, i.e., j and k. The implementation of the approach to automated manufacturing systems requires guidelines in selection of point T based on two criteria:

(a). *Distance between points* A and T. Point T should be located as close as possible to point A and preferably on the same part to avoid or minimize any error in the relative distance variation between A and T in the non-measured direction of point A.
(b). *Feature tracing ability* requirements for point T.

Following the results for the feature-based measurement error model presented in Section 3 and the definitions shown in Fig. 9, guidelines for the selection of point T to compensate measurement point A (level 3—point feature) with non-zero angles for α and β are summarized in Table 3 (for α and β angles between -45° to 135° these relations also hold if 180° is added).

In the case where the α or β angles are close to zero or 90° (Fig. 9), the guidelines can be simplified as presented in Table 4.

Step 2. Use measurements of point T in the non-measured direction(s) j (and/or k) at point A to calculate the feature of point A deviation δA_j (and/or δA_k) in direction j (and/or k).

Step 3. Use Equations (5)–(7) to determine the impact (compensation value) of δA_j (and/or δA_k) on the measurement results of point A in measured direction i.

Step 4. Adjust/compensate each measurement of point A using the computed compensation value.

Example: An example of relations between measurement points pair {A, T} used to compensate the feature-based measurement error of point A is shown in Fig. 16. This

Table 3. Guidelines for selection of point T to compensate feature-based measurement error of point A

α	β	*Measurement reported in direction (measurement point A)*	*Accurate measurement necessary in direction (measurement point T)*
$[-45^\circ, 45^\circ]$	$[-45^\circ, 45^\circ]$	y	z and x
$[-45^\circ, 45^\circ]$	$[45^\circ, 135^\circ]$	x	y and z
$[45^\circ, 135^\circ]$	Any	z	x and y

Table 4. Guidelines for selection of point T to compensate feature-based measurement error of point A: special cases for α and $\beta = \{45^\circ, 90^\circ, 135^\circ, 180^\circ\}$

α	β	*Measurement reported in direction (measurement point A)*	*Accurate measurement necessary in direction (measurement point T)*
$[-45^\circ, 45^\circ]$	0	y	z
$[-45^\circ, 45^\circ]$	90°	x	z
$[45^\circ, 135^\circ]$	90°	z	x
0	$[-45^\circ, 45^\circ]$	y	x
0	$[45^\circ, 135^\circ]$	x	y
90	Any	z	None

example corresponds to the first case example presented in Table 4.

6.2.2. *Industrial case study 2*

A single measurement point (point feature-level 3) located on the A-pillar door flange of the automotive body was analyzed for feature-based measurement error estimation and implementation of the proposed error compensation method. The point is shown in Fig. 17 and is marked as "plane". This point is measured by a CMM and was selected by design and manufacturing engineers as one of the key product characteristic (KPC) measurement points with an assigned tolerance of ± 1.0 mm. The measurements at this point are used to evaluate the front-door fitting process; that is the relative position and orientation of front door in relation to the door opening as measured by gap and flushness parameters. The door fitting process is one of the most critical quality concerns during the automotive body assembly process. The selected measurement point can be characterized using a CAD model as:

1. Measurement point A = "plane."
2. Point feature (level 3) with measurement direction perpendicular to the measured surface.
3. $\alpha = 26.15^\circ$ (y-z plane) and $\beta = 0.69^\circ$ (x-y plane).
4. Measurements that are reported in the y direction.
5. Non-traceable directions: x and z, since $\alpha > 0$ and $\beta > 0$.

We will illustrate the implementation of the feature-based measurement error compensation approach using the four-step procedure presented in Section 6.2.

Step 1. Selection of traceable measurement point T.
The selected point should be traceable in the x and z directions. The closest traceable measurement point on the front door opening are presented in Fig. 17 and marked as T = {"hole", "slot"}. Since the measurement point "hole" is not only located closer to the investigated point "plane;" but is also located on the same part (the A-pillar), then the measurement point T = "hole" was selected for compensation of the point A = "plane"

Step 2. Measurement of the point T = "hole" in the x and z directions was used to estimate the deviation of

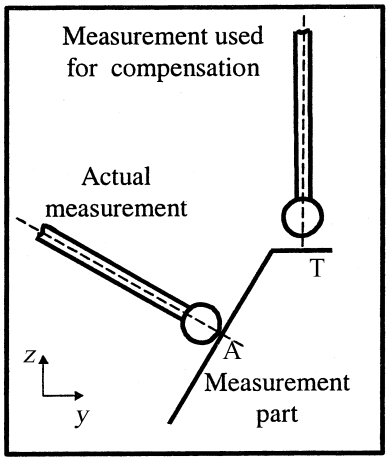

Fig. 16. An example of the relationships between a pair of measurement points [A, T]. Point A—actual measurement; Point T—measurement point used for compensation of the point A deviation in the z direction.

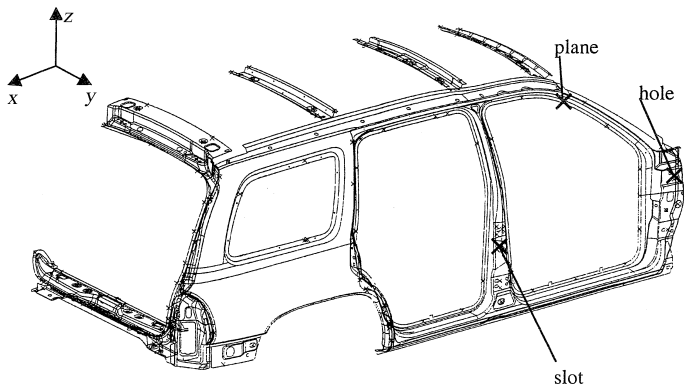

Fig. 17. Industrial case study 2: the feature-based measurement error for truck cab measurement point (point feature-level 3). Point A—measurement point marked as "plane" (level 3); and Point T—measurement point marked as "hole" (level 1) used for the compensation of the point A deviation in the z direction.

the point A = "plane" (δA_x and δA_z) in the non-measured directions (x and z).

Step 3. Equation (6) was used to calculate $e_3(y)$ for point A = "plane".
The feature-based measurement error for these measurement points was estimated as $e_3(y) = 0.74$ mm (37% of the tolerance window).

Step 4. The measurement results of the point A = "plane" was compensated by δA_x and δA_z obtained from the measurement of point T = "hole."

By deriving and processing the information about the deviation of point A = "plane," the measurement of this point could be used to compensate for the error resulting in a change from 0.74 to 0.61 mm (a 18% decrease).

The presented case study shows that feature-based measurement error can be partially compensated by analyzing a measurement point pair {A, T} instead of a single measurement point A. Additionally, this may also lead to a better selection of the measurement points (sensor layout optimization) and increase the utilization of dimensional information for in-line/off-line process control and improvement (Khan *et al.*, 1999; Ding *et al.*, 2003).

7. Conclusions

Dimensional measurements based on coordinate metrology are widely used for design verification, process control and diagnostics in various manufacturing processes. However, CMSs (mechanical or optical CMMs) have inherent errors due to the lack of a tracing ability for some of the measured features, which are important for process control and variation reduction in automated manufacturing systems. The lack of a feature tracing ability means that instead of measuring a given feature, the CMS may actually measure the area around the selected feature.

In this paper, a feature-based measurement error model is developed to estimate the measurement error caused by the aforementioned deficiency. The feature-based measurement error is independent of the CMM error. The presented analysis shows the impact of the feature-based measurement error on the overall accuracy of measurements. The industrial case studies on the automotive assembly process show that feature-based measurement error affects about 35–65% of the selected measurement points. Additionally, for 20% of all the measurement points, feature-based error causes 4% or higher errors. This paper develops a feature-based measurement error model for different measurement conditions such as: type of feature, direction of measurement, geometry of feature and mislocation error. It also presents a feature-based measurement error map and error compensation approach. Simulations and two case studies illustrate the proposed method.

The presented feature-based measurement error is related to and extends the research on the areas of measurement traceability and task-specific measurement uncertainty by providing insights into what could be called feature-based metrology.

Acknowledgement

The authors acknowledge the financial support provided by the National Science Foundation under DMI-0218208, API Inc. and State of Wisconsin's Industrial and Economic Development Research Fund (IEDR) program.

References

Abbe, M., Takamasu, K. and Ozono, S. (2000) Reliability of parametric error on calibration, in *Proceedings of the IMEKO 2000 International Measurement Confederation XVI IMEKO World Congress*, Vienna, Austria, Sept. 25–28, 180–184.

Anon. (1988) *Operator Friendly Interface* (*OFI*) *Reference Manual. Manual No. 58004135*, Sheffield.

Anon. (1992) *Master Measuring System User Manual, Code: M1U104EI*, 5th edn., DEA, Grugliasco, Italy.

Anon. (1994) *Perceptron DSP 2000 System Manual*, Perceptron, Plymouth, MI.

Anon. (1995) *Guide to the Expression of Uncertainty in Measurements* (*GUM*), International Organization for Standards (ISO), Geneva, Switzerland.

Asada, H. and By, A. (1985) Kinematic analysis of workpart fixturing for flexible assembly with automatically reconfigurable fixtures. *IEEE Journal of Robotics and Automation*, **1/2**, 86–94.

Bosch, J.A. (1995) *Coordinate Measuring Machines and Systems*, Marcel Decker, New York, NY.

Bryan, J. (1990) International status of thermal error research. *Annals of the CIRP*, **39**(2), 645–656.

Ceglarek, D. (1998) Multivariate analysis and evaluation of adaptive sheet metal assembly systems. *Annals of the CIRP*, **47**(1), 17–22.

Ceglarek, D. and Shi, J. (1995) Dimensional variation reduction for automotive body assembly. *Manufacturing Review*, **8**(2), 282–294.

Ceglarek, D. and Shi, J. (1996) Fixture failure diagnosis for the autobody assembly using pattern recognition. *Transactions of the ASME, Journal of Engineering for Industry*, **118**(1), 55–66.

Ceglarek, D., Shi, J. and Wu, S.M. (1994) A knowledge-based diagnosis approach for the launch of the autobody assembly process. *Transactions of the ASME, Journal of Engineering for Industry*, **116**(4), 491–499.

Ding, Y., Ceglarek, D. and Shi, J. (2000) Modeling and diagnosis of multistage manufacturing processes: part II diagnosis, in *Proceedings of the 2000 Japan/ USA Symposium on Flexible Automation*, Ann Arbor, MI, July 23–26.

Ding, Y., Ceglarek, D. and Shi, J. (2002a) Fault diagnosis of multistage manufacturing processes by using state space approach. *ASME Transactions, Journal of Manufacturing Science and Engineering*, **124**(2), 313–322.

Ding, Y., Shi, J.J. and Ceglarek, D. (2002b) Diagnosability analysis of multi-station manufacturing processes. *ASME, Journal of Dynamic Systems Measurement and Control*, **124**(1), 1–13.

Ding, Y., Ceglarek, D. and Shi, J. (2002c) Design evaluation of multi-station assembly processes by using state space approach. *ASME, Journal of Mechanical Design*, **124**(3), 408–418.

Ding, Y., Kim, P., Ceglarek, D. and Jin, J. (2003) Optimal sensor distribution for variation diagnosis in multi-station manufacturing processes. *IEEE Transactions on Robotics and Automation*, **19**(4), 543–556.

Eman, K.F., Wu, B.T. and De Vries, M.F. (1987) A generalized geometric error model of multi-axis machines. *Annals of the CIRP*, **36**(2), 253–256.

Estler, W.T., Phillips, S.D., Borchardt, B., Hopp, T., Witzgall, C., Levenson, M., Eberhardt, K., McClain, M., Shen, Y. and Zhang, X. (1996) Error compensation for CMM touch trigger probes. *Precision Engineering*, **19**(2), 85–97.

Greer, D. (1988) On-line machine vision sensor measurements in a coordinate system. SME Paper IQ88-289, Society of Manufacturing Engineers, Dearborn, MI.

Haitjema, H., Van Dorp, B.W.J.J.A., Morel, M.A.A. and Schellekens, P.H.J. (2002) Task specific uncertainty estimation in dimensional metrology, in *Proceedings of the 3rd International Euspen Conference*, Delbressine, Schellekens, Homburg and Haitjema (eds.), Eindhoven, The Netherlands, pp. 613–616.

Hernla, M. (1997) Task specific uncertainty in coordinate measurement. *Technisches Messen*, **64**(7–8), 286–293.

Hocken, R., Raja, J. and Babu, U. (1993) Sampling issues in coordinate metrology. *Manufacturing Review*, **6**(4), 282–294.

Hocken, R., Simpson, J.A., Borchardt, B., Lazar, J., Reeve, C. and Stein, P. (1977) Three dimensional metrology. *Annals of the CIRP*, **26**(2), 403–408.

Hopp, T.H. (1993) Computational metrology. *Manufacturing Review*, **6**(4), 295–304.

Hu, S. and Wu, S.M. (1992) Identifying root causes of variation in automobile body assembly using principal component analysis. *Transactions of NAMRI*, **XX**, 311–316.

Jin, J. and Shi, J. (1999) State space modeling of sheet metal assembly for dimensional control. *ASME, Journal of Manufacturing Science and Engineering*, **121**(4), 756–762.

Khan, A., Ceglarek, D., Shi, J., Ni, J. and Woo, T.C. (1999) Sensor optimization for fault diagnosis in single fixture system: a methodology. *ASME, Journal of Manufacturing Science and Engineering*, **121**(1), 109–117.

Lee, G, Mou, J. and Shen, Y. (2000) Decoupling the confounded effect of machine error and geometric characteristics of artifacts in precision measurement and machine calibration. *Transactions of the ASME, Journal of Manufacturing Science and Engineering*, **122**, 331–337.

Menassa, R.J. and DeVries, W.R. (1989) Locating point synthesis in fixture design. *Annals of the CIRP*, **38**(1), 165–169.

Montgomery, D.C. (1997) *Introduction to Statistical Quality Control*, 3rd edn., Wiley, New York, NY.

Morgan, D.E., Piazza, J.E. and Plyler, R.E. (1984) Inherent errors on X, Y, Z coordinate measuring machines on curved surfaces, in *Proceedings of the 1984 Annual International Industrial Engineering Conference*, Chicago, IL, May 6–10, pp. 400–405.

Nair, V., Hansen, M. and Shi, J. (2000) Statistics in advanced manufacturing. *Journal of the American Statistical Association*, **95**(451), 1002–1005.

Nawara, L. and Kowalski, M. (1985) Influence of the multicoordinate measuring machine head characteristic on circular profiles measurements. *Annals of the CIRP*, **34**(1), 449–453.

Phillips, S.D. (1995) Performance evaluations, in *Coordinate Measuring Machines and Systems*, Bosch, J.A. (ed.), Marcel Decker, New York, NY, ch. 7.

Salisbury, E.J. and Peters, F.E. (1998) The impact of surface errors on fixtured workpiece location and orientation. *Transactions of the NAMRI/ SME*, **XXVI**, 323–328.

Soons, J.A., Theuws, F.C. and Schellekens, P.H. (1992) Modeling the errors of multi-axis machines: a general methodology. *Precision Engineering*, **14**(1), 5–19.

Wilhelm, R.G., Hocken, R. and Schwenke, H. (2001) Task specific uncertainty in coordinate measurement. *Annals of the CIRP*, **50**(2), 553–563.

Yan, Z., Yang, B. and Menq, C. (1999a) Uncertainty analysis and variation reduction of three dimensional coordinate metrology. Part 1: geometric error decomposition. *International Journal of Machine Tools and Manufacturing*, **39**, 1199–1217.

Yan, Z., Yang, B. and Menq, C. (1999b) Uncertainty analysis and variation reduction of three dimensional coordinate metrology. Part 2: uncertainty analysis. *International Journal of Machine Tools and Manufacturing*, **39**, 1219–1238.

Yan, Z., Yang, B. and Menq, C. (1999c) Uncertainty analysis and variation reduction of three dimensional coordinate metrology. Part 3: variation reduction. *International Journal of Machine Tools and Manufacturing*, **39**, 1239–1261.

Yuan, J.X. and Ni, J. (1998) The real-time error compensation technique for CNC machining systems. *Mechatronics*, **8**(4), 359–380.

Zhang, G., Veale, R., Charlton, T., Borchardt, B. and Hocken, R. (1985) Error compensation of coordinate measuring machines. *Annals of the CIRP*, **34**(1), 445–448.

Biographies

Wenzhen Huang is a Research Assistant/Ph.D. student in the Industrial Engineering Department at the University of Wisconsin-Madison. He graduated in Mechanical Engineering from Shanghai Jiaotong University, China, in 1987. His current research includes multistage manufacturing process modeling and diagnostic. He is involved in research projects funded by major automobile companies in the United States. He has received Best Graduate Student Paper Awards by INFORMS Quality, Statistics and Reliability Section in 2002. He is a member of ASME, IIE and INFORMS.

Zhenyu Kong is a Research Assistant/Ph.D. student in the Industrial Engineering Department at the University of Wisconsin-Madison. He received his B.S. and M.S. in Mechanical Engineering from Harbin Institute of Technology, China, in 1993 and 1995, respectively. His current research includes reconfigurability and reusability of multistage assembly processes. He is a member of ASME, IIE and INFORMS.

Dariusz (Darek) Ceglarek received his Ph.D. in Mechanical Engineering from the University of Michigan, Ann Arbor in 1994. Dr. Ceglarek is currently an Associate Professor in the Industrial Engineering Department at the University of Wisconsin-Madison. His research expertise is in dimensional analysis of manufacturing processes, in-process quality control and improvement in manufacturing, design for manufacturability (fusion of design, manufacturing and statistics), and automated on-line diagnosis and monitoring. His research interests include design, control and diagnostics of multistage manufacturing processes; developing statistical methods driven by engineering models to achieve quality improvement; modeling and analysis of product/process key characteristics causality; and reconfigurable/reusable assembly systems. His current research is sponsored by the National Science Foundation, DaimlerChrysler Corp., DCS, and State of Wisconsin's IEDR Program. Dr. Ceglarek was elected as a corresponding member of CIRP and is a member of ASME, SME, NAMRI, IIE, and INFORMS. He has received a number of awards for his work including the 2003 CAREER Award from the NSF, 1998 Dell K. Allen Outstanding Young Manufacturing Engineer Award from the Society of Manufacturing Engineers (SME) and two Best Paper Awards by ASME MED and DED divisions in 2000 and 2001, respectively. For more information: http://www.cae.wisc-edu/ndarek

Emilio Brahmst is an Engineering Consultant in the Center for Automotive Research, ERIM. He holds a Master's Degree in Mechanical and Production Engineering from the Technical University of Berlin, Germany, and a Master's Degree in Manufacturing from the University of Michigan. He graduated in Production Technology from Technical University of Berlin, Germany, in 1996. His current research includes quality control and assurance of automobile body assembly systems and stamping operations. He is involved in research projects funded by major automobile companies in the United States. He is a member of SME.